Supporting Information

A highly sensitive TTF-functionalised probe for the determination of physiological thiols and its application in tumor cells

Wei Wang,*[a] Na Zhao,[a] Yan Geng,[b] Shi-Bin Cui,[a] Jürg Hauser,[b] Silvio Decurtins[b] and Shi-Xia Liu*[b]

1. Apparatus and Materials

Apparatus: Air and/or water-sensitive reactions were conducted under Ar in dry, freshly distilled solvents. Elemental analyses were performed on an EA 1110 Elemental Analyzer CHN Carlo Erba Instruments. ^{1}H and ^{13}C NMR spectra were acquired on a Bruker Avance 300 spectrometer operating at 300 MHz for ^{1}H and 75.5 MHz for ^{13}C. Chemical shifts are reported in parts per million (ppm) and are referenced to the residual solvent peak (DMSO-d_6, ^{1}H = 2.50 ppm, ^{13}C = 39.6 ppm). Coupling constants (*J*) are given in hertz (Hz) and are quoted to the nearest 0.5 Hz. Peak multiplicities are described in the following way: singlet (s), triplet (t) and multiplet (m). UV-vis absorption spectrum was recorded on a Perkin-Elmer Lambda 900. FT-IR spectra were recorded on a Perkin–Elmer One FT-IR spectrometer. Melting points were determined on a Büchi melting point apparatus and are uncorrected. High-resolution mass spectrum was recorded with ESI (electrospray ionization) on a Thermo Scientific LTQ Orbitrap XL in the positive mode. Cyclic voltammetry was conducted on a PGSTAT 101 potentiostat. An Ag/AgCl electrode containing 2 M LiCl (in ethanol) served as reference electrode, a glassy carbon electrode as counter electrode, and a Pt-disk as working electrode. Cyclic voltammetric measurements were performed at room temperature under Ar in CH_2Cl_2 (1×10^{-4} M) with 0.1 M *n*-Bu_4NPF_6 as supporting electrolyte at a scan rate of 100 mV/s.

Crystallography: A single crystal of **1** was mounted with Paratone on a glass needle and used for X-ray structure determination at 173 K. All measurements were made on an Oxford Diffraction SuperNova area-detector diffractometer[1] using mirror optics monochromated MoK_α radiation (λ = 0.71073 Å). The unit cell constants and an orientation matrix for data collection were obtained from a least-squares refinement of the setting angles of 2975 reflections in the range 2.41° < θ < 25.63°. A total of 1152 frames were collected using ω scans, 60 seconds exposure time and a rotation angle of 1.0° per frame, and a crystal-detector distance of 66.2 mm. Data reduction was performed using the CrysAlisPro[1] program. The intensities were corrected for Lorentz and polarization effects, and an absorption correction based on the multi-scan method using SCALE3 ABSPACK in CrysAlisPro[2] was applied. The structure was solved by direct methods using SIR97, [2] which revealed the positions of all non-hydrogen atoms. The non-hydrogen atoms were refined anisotropically. All H-atoms were placed in geometrically calculated positions and refined using a riding model where each H-atom was assigned a fixed isotropic displacement parameter with a value equal to 1.2 Ueq of its parent atom atom (1.5 Ueq for the methyl group). Refinement of the structure was carried out on F^2 using full-matrix least-squares procedures, which minimized the function $\Sigma w(F_o^2 - F_c^2)_2$. The weighting scheme was based on counting statistics and included a factor to downweight the intense reflections. All calculations were performed using the SHELXL-97[3] program.

Electrochemical behaviour of probe 1 in the presence and absence of GSH: All the electrochemical experiments were performed with a CHI 832B electrochemical analyzer (Shanghai CHI Instrument Company, China) using a three-electrode system composed of a Au electrode (diameter: 2.0 mm) as a working electrode, Ag/AgCl/ (saturated) KCl as a reference electrode, and Pt wire as an auxiliary electrode. All the experimental solutions were deoxygenated by bubbling nitrogen for 20 min, and a nitrogen atmosphere was kept over the solutions during measurements. The pH value was measured with a PB-10 Precision pH meter (Shanghai Precision & Scientific Instrument Co., Ltd., Shanghai, China).

Materials: Unless stated otherwise, all reagents were purchased from commercial

sources and used without additional purification. 5,6-Diamino-1,3-benzodithiole-2-thione (**3**),[4] and 4,5-bis(propylthio)-1,3-dithiole-2-one,[5] were prepared according to literature procedures.

2. Synthesis and Characterisation

[1,3]Dithiolo[4,5-f]-2,1,3-benzoselenadiazole-6-thione (**2**): The mixture of **3** (642 mg, 3 mmol) and SeO_2 (333 mg, 3 mmol) was ground in a mortar for 1h. During the reaction, cyclohexane was added dropwise to keep the mixture moist. Afterward, the crude product was purified by column chromatography on silica gel using dichloromethane as eluent to afford **2** as a red solid. Yield: 600 mg (73%); m.p. 282-283 °C; IR (KBr): $\tilde{\nu}$ = 3436, 2920, 1631, 1384, 1092, 576 cm^{-1}; ^1H NMR (300 MHz, DMSO-d_6): δ = 8.40 (s) ppm; ^{13}C NMR (75 MHz, DMSO-d_6): δ = 231.8, 157.4, 143.1, 115.3 ppm; HRMS (ESI): *m/z* calcd for $C_7H_3N_2S_3Se$: 289.8618; found: 289.8633 (M+1); elemental analysis calcd (%) for $C_7H_2N_2S_3Se$: C 29.07, H 0.70, N 9.68; found: C 29.11, H 0.70, N 9.19.

2-[4,5-Bis(propylsulfanyl)-1,3-dithiol-2-ylidene][1,3]dithiolo[4,5-f]-2,1,3-benzoselenadiazole (**1**): Triethylphosphite (8 mL) was added to the mixture of **2** (145 mg, 0.5 mmol) and 4,5-bis(propylthio)-1,3-dithiole-2-one (333 mg, 1.25 mmol) in toluene (3 mL) under Ar. The mixture was refluxed at 120 °C for 3 h before cooling to room temperature. After filtration, the precipitate was collected and washed with MeOH. Then the crude product was purified by column chromatography on silica gel using hexane:dichloromethane = 1:1 (v/v) as eluent to afford compound **1** as a dark red solid. Yield: 90 mg (33%); m.p.: 146-147 °C; IR (KBr): $\tilde{\nu}$ = 3436, 2958, 1636, 1457, 1418, 1347, 1266, 1072, 886, 837, 773, 749, 730 cm^{-1}; ^1H NMR (300 MHz, DMSO-d_6): δ = 8.04 (s, 2H), 2.85-2.90 (t, 4H), 1.56-1.64 (m, 4H), 0.95-1.00 (t, 6H); ^{13}C NMR (75 MHz, DMSO-d_6): δ = 158.8, 143.4, 127.8, 116.7, 113.0, 107.8, 38.3, 23.1, 13.1 ppm; HRMS (ESI): *m/z* calcd for $C_{16}H_{16}N_2S_6Se$: 507.8803; found: 507.8870.

NMR Spectra of **2**

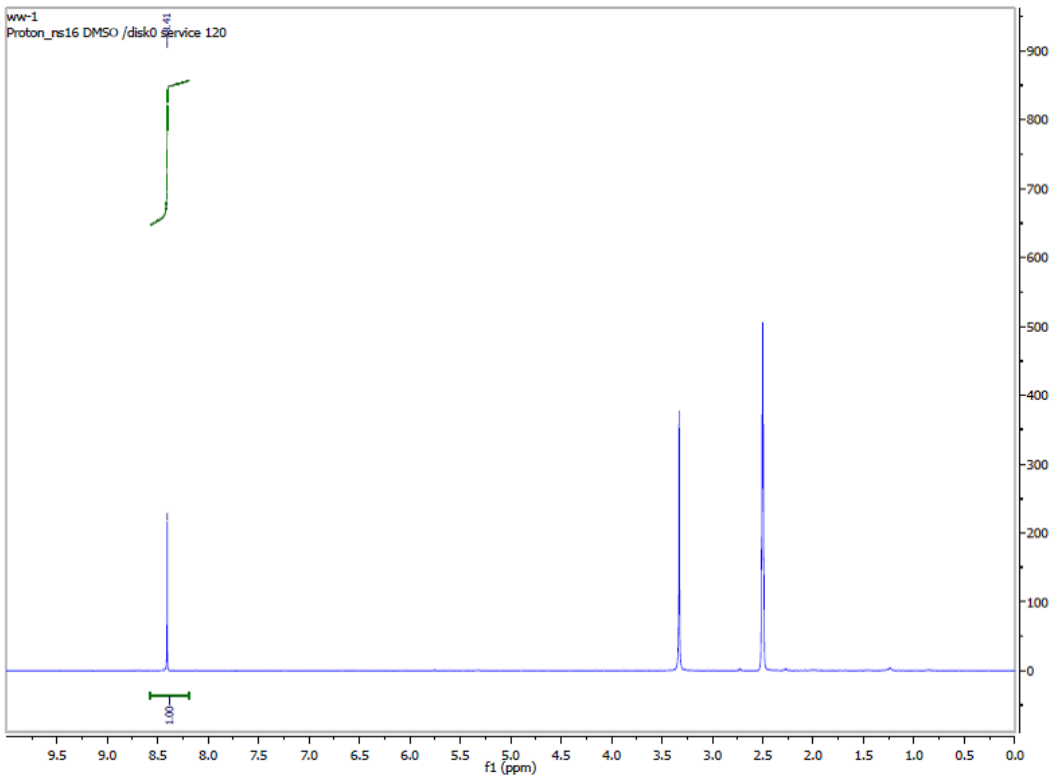

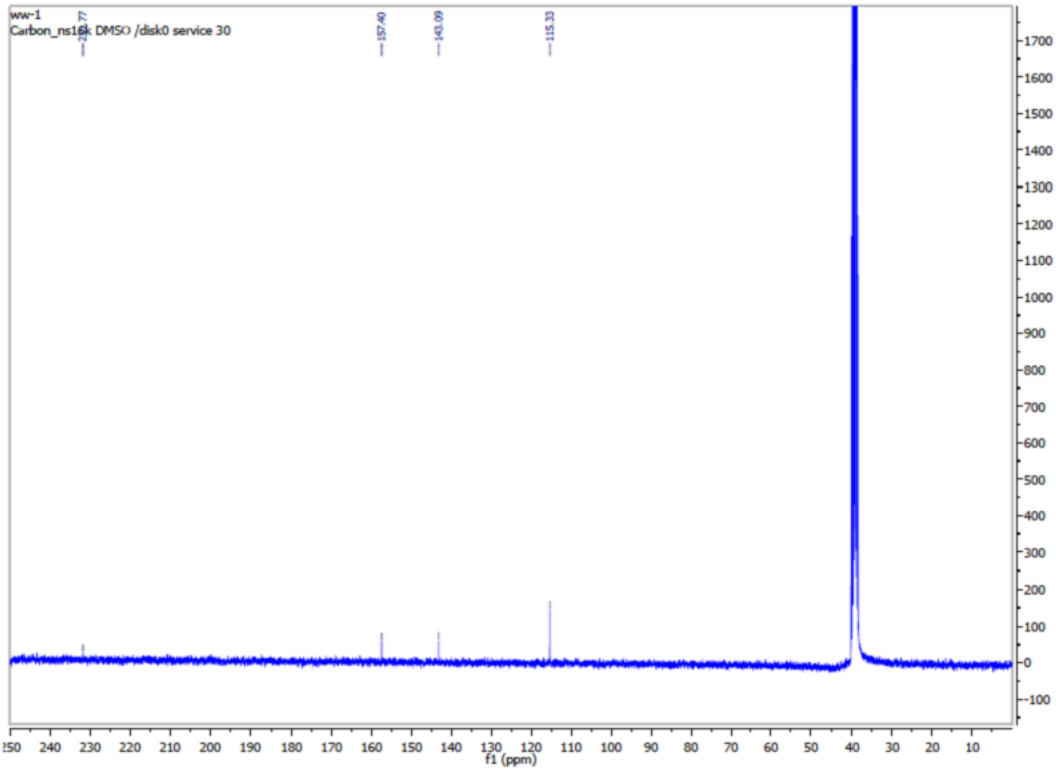

NMR Spectra of **1**

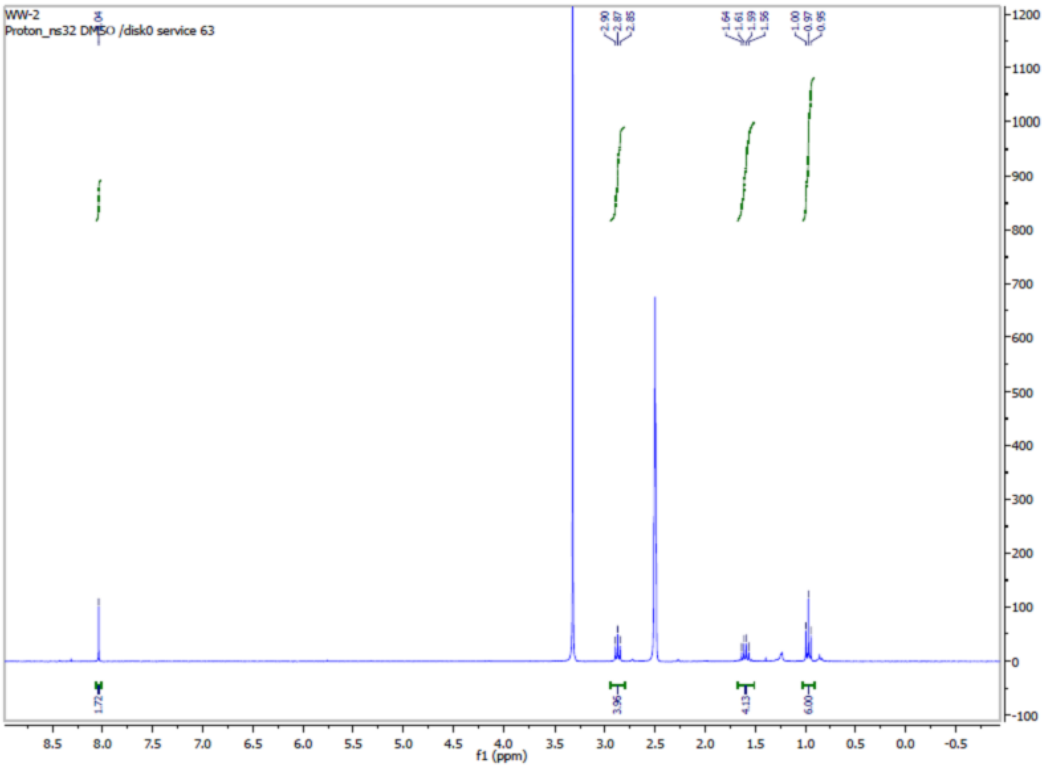

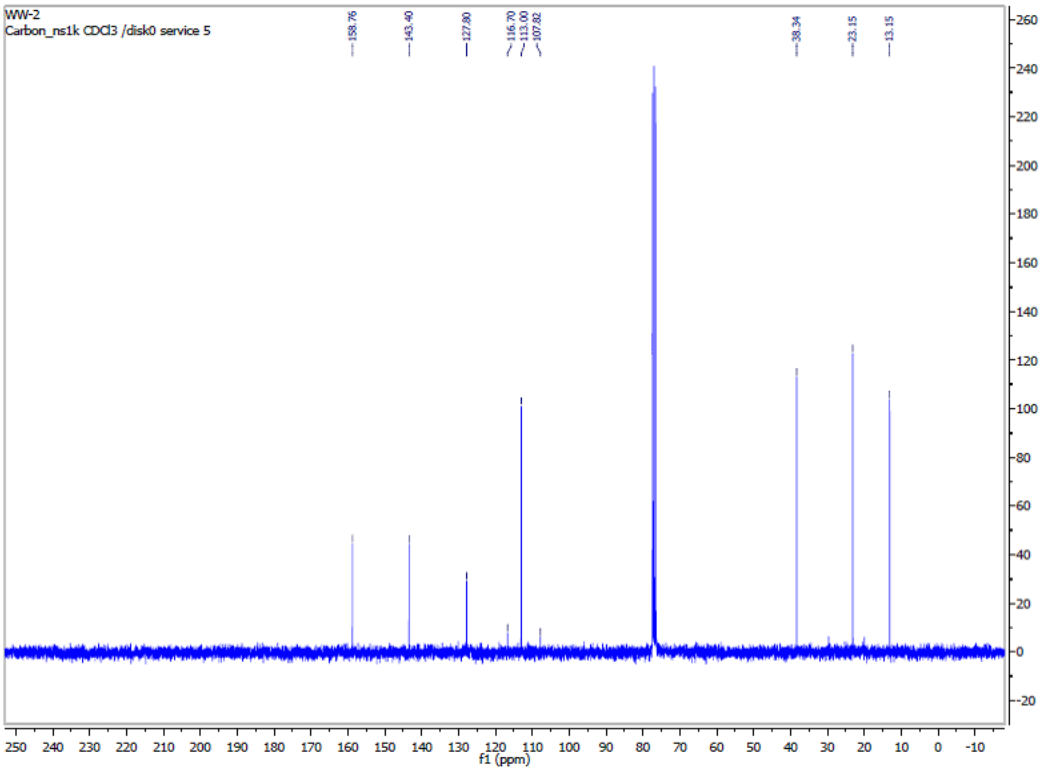

Table S1. Crystallographic data for probe **1**·$(C_6H_{14})_{0.5}$.

	1·$(C_6H_{14})_{0.5}$
Formula	$C_{19}H_{23}N_2S_6Se$
Formula weight	550.71
Crystal system	Monoclinic
Space group	*P2(1)/c*
a (Å)	15.8030(3)
b (Å)	16.5945(2)
c (Å)	9.10215(12)
α (°)	90
β (°)	102.1603(17)
γ (°)	90
V (Å^3)	2333.42(6)
Z	4
ρ_{calc} (g/cm^3)	1.568
μ (mm^{-1})	2.155
Temperature (K)	173(2)
No. Refl.	25589
R_1; wR_2 [$I > 2\sigma(I)$]	0.0446; 0.1003

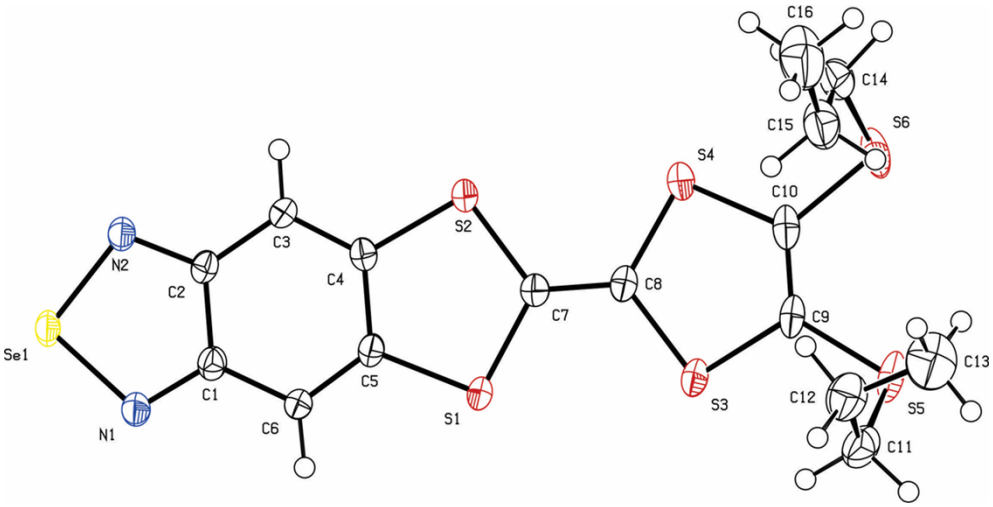

Figure S1. ORTEP view of the molecule **1**.

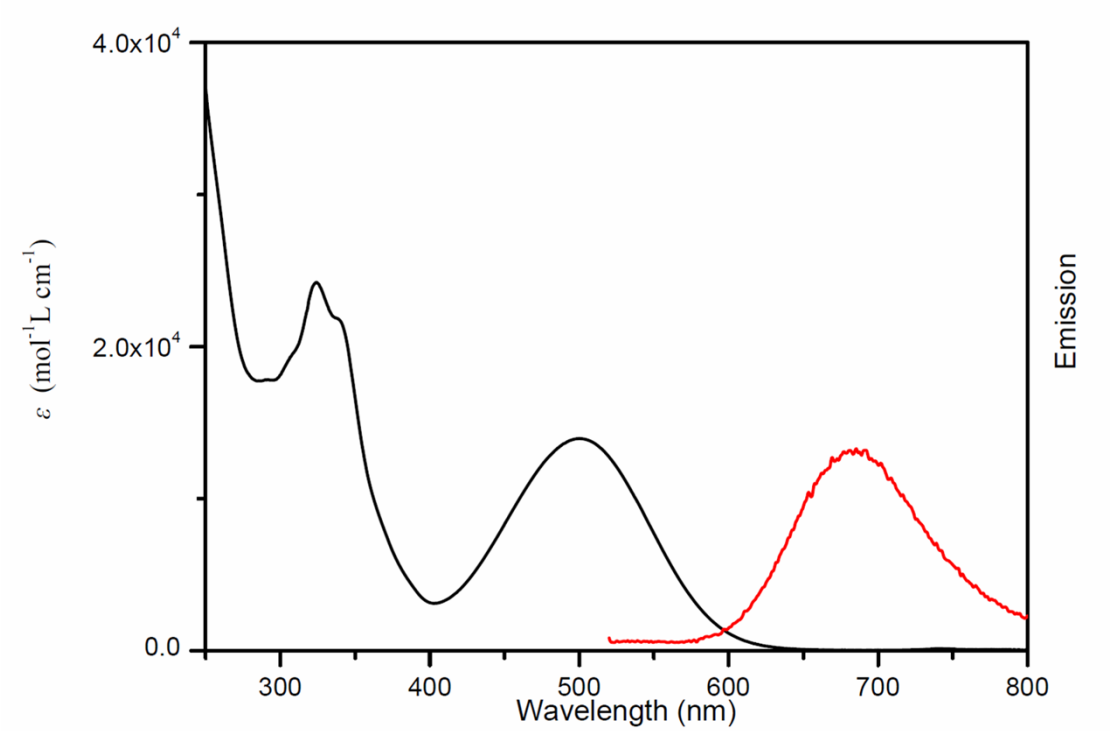

Figure S2. Absorption and emission spectra of probe **1** (λ_{ex} = 500 nm) in THF solution at room temperature.

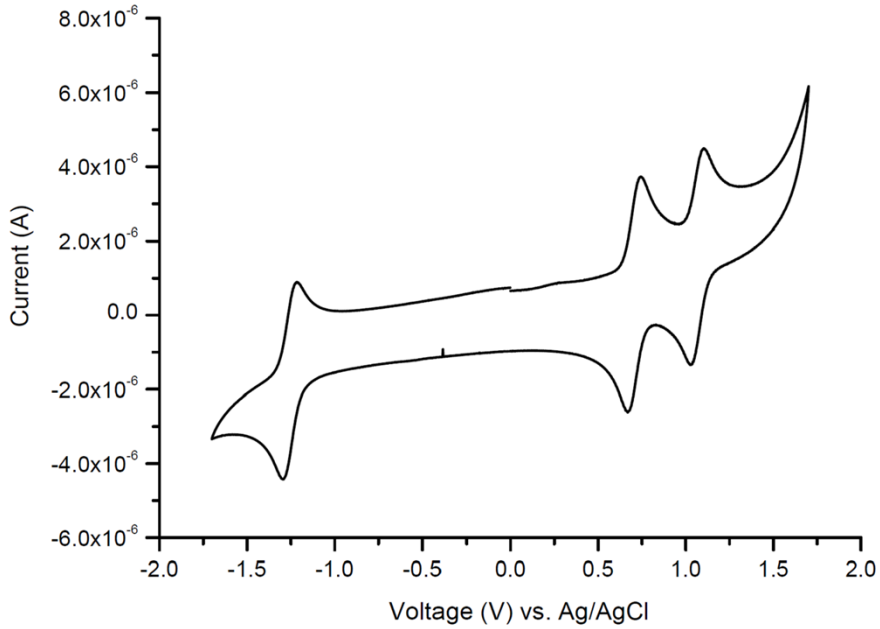

Figure S3. Cyclic voltammogram of probe **1**, recorded in a mixture of CH_2Cl_2 with *n*-Bu_4NPF_6 (0.1 mol dm^{-3}) as the supporting electrolyte.

Table S2. Optical and electrochemical data, HOMO and LUMO energy levels of probe **1**.

	λ_{abs} (nm) (ε_{max}(10^4 M^{-1} cm^{-1}))	λ_{em} (nm)	$E_{g,opt}$[a] (eV)	$E_{1/2}$[b] (V)	$E_{1/2}$[b] (V)	HOMO[c] (eV)	LUMO[d] (eV)
probe **1**	498 (1.39)	680	2.08	0.21	-1.75	-4.93	-3.13

[a] Optical band gap is estimated from the cross point of UV-vis absorption and emission spectra. [b] The oxidation potential of Fc^+/Fc against Ag/AgCl was recorded in CH_2Cl_2-Bu_4NPF_6 (0.1 M) solution to be 0.49 V, therefore the herein half-wave potentials are converted to Fc/Fc^+ by subtracting 0.49 V from Ag/AgCl values. [c] HOMO level is calculated from the onset of the first oxidation potential in cyclic voltammetry, according to the equation $E_{HOMO} = [-e(E_{onset,\ ox} -0.49 + 4.8)]$ eV, where 4.8 eV is the energy level of ferrocene below the vacuum level. [d] LUMO level is calculated from the onset of the first reduction potential in cyclic voltammetry, according to the equation $E_{LUMO} = [-e(E_{onset,\ red} -0.49 + 4.8)]$ eV, where 4.8 eV is the energy level of ferrocene below the vacuum level.

3. The Electrochemical Behaviour of Probe 1

Cyclic voltammogram of probe **1** (25.2 μM) was performed on an Au electrode (diameter: 2.0 mm) in 0.2 M BR buffer solution (pH 2.0) at room temperature in the potential range of 0.5 V ~ -0.4 V, followed by adding different concentrations of GSH (0, 0.5, 1.0, 5.0 nM) for 20 min reaction time. Scan rate: 100 mV/s. The cyclic voltammograms of probe **1** in the absence and presence of GSH were shown in Fig. S4.

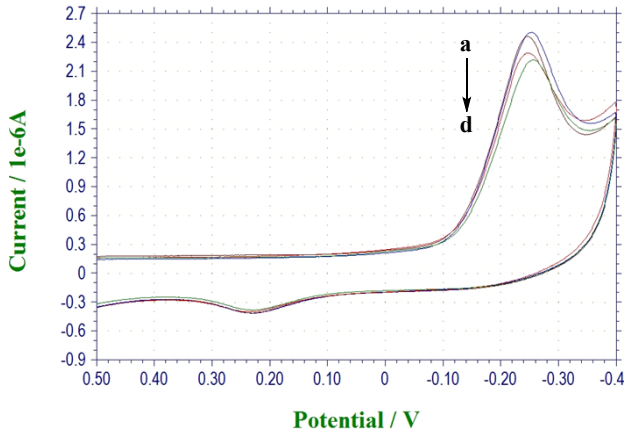

Figure S4. Cyclic voltammograms of probe **1** toward different concentrations of GSH (final concentrations: a→d: 0, 0.5, 1.0, 5.0 nM) after incubation at 25 °C for 20 min in 0.2 M BR (pH 2.0).

In order to demonstrate the reaction of protons involved in the electrode process, the E-pH experiment was carried out. The effect of pH value of the BR buffer solution on the reduction peak potential (Ep) of probe **1** was investigated in a pH range from 1.5 to 4.0 (Fig. S5). The pH increase caused the negative shift of the reduction peak potential of probe **1**. A linear regression equation of Ep with pH as Ep = 0.046 - 0.074 pH was obtained with a correlation coefficient of γ = 0.9916 (Fig. S6). So, the number of protons participating in the reaction is approximately equal to the electron transfer number. The results are in good agreement with the previously reported ones.

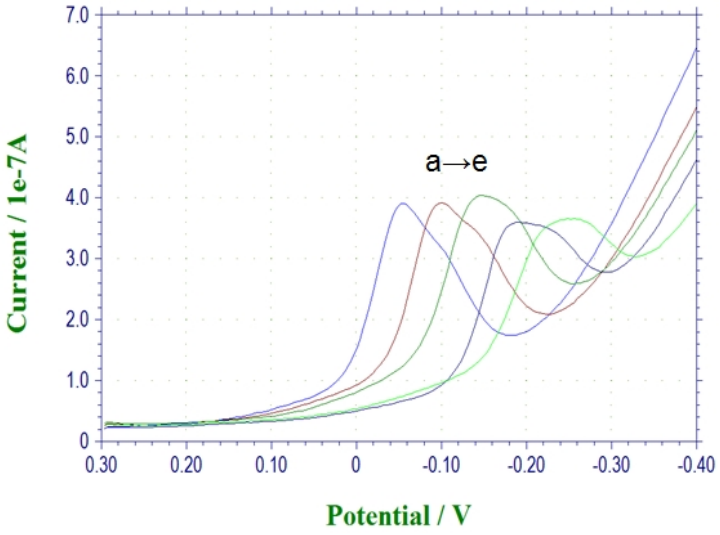

Figure S5. The effect of pH value on the reduction peak potential (Ep) of **1** at c = 12.5 μM (pH: a→e: 1.5, 2.0, 2.5, 3.0, and 4.0).

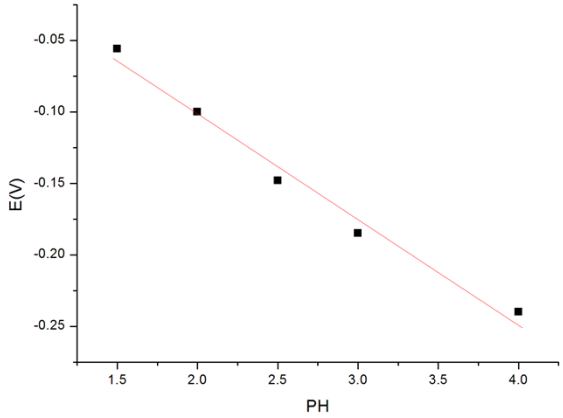

Figure S6. The potential (Ep) dependence of **1** with pH. Solid line represents the linear regression: Ep = 0.046 - 0.074 pH (correlation coefficient of γ = 0.9916).

As shown in Scheme 2, after the reduction at the electrode, probe **1** was converted to a product containing the TTF-fused *o*-phenylene-diamine (TTF-OPD) moiety, which can be oxidized at the electrode. The DPV experiment was implemented to testify the yielding of the TTF-OPD-moiety from the electrochemical reduction of probe **1**. It can be seen from Figure S7 that the direct anodic scan of **1** from 0.0 V to 0.5 V yields no peaks (blue curve in Fig. S7), while a pre-reduction of probe **1**, firstly executed on the electrode surface from 0.3 V to -0.4 V, results in one oxidation peak (red curve in Fig. S7). This observation is consistent with the results from cyclic voltammetric experiments. As shown in cyclic voltammograms of probe **1** (Fig. S4), an anodic peak at 0.232 V was observed. Compared to our previous results based on the piazselenole probe,[6] the presence of TTF induced a significant negative shift of this anodic peak corresponding to the oxidation of the resulting TTF-fused o-phenylene-diamine (TTF-OPD) moiety.

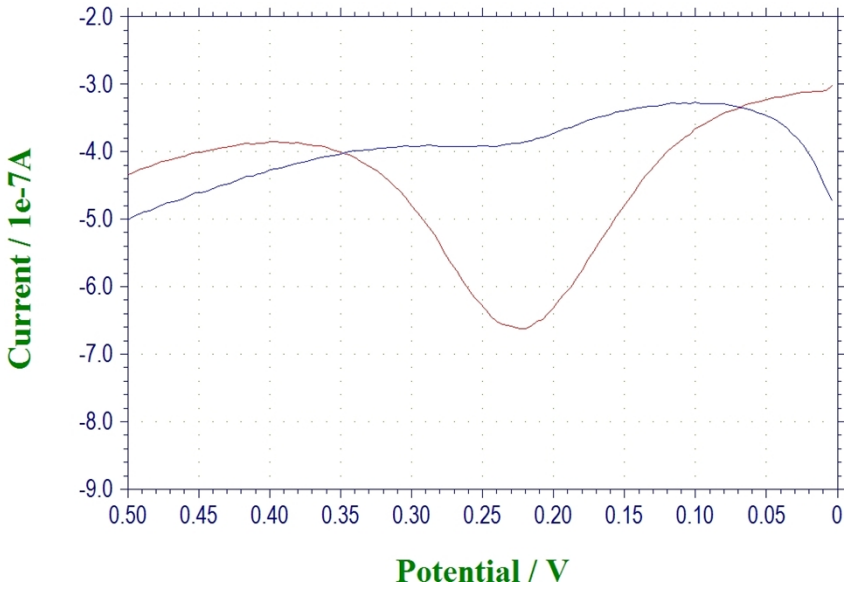

Figure S7. Differential pulse voltammograms of 25.2 μM probe **1** obtained in 0.2 M BR buffer (pH 2.0) without (blue) and with (red) a preconditioning by a single negative scan.

4. Optimization of Experimental Variables

The effect of some experimental variables was tested with the reaction of probe **1** and GSH.

4.1 Effect of the pH value of BR

In the experiment, the pH of BR has a great effect on the decrease of the peak current (ΔI_P) of probe **1**. A series of BR buffers with different pH values were tested (Fig. S8). It can be seen that the ΔI_P of probe **1** increases when the pH varies from 1.5 to 2.0 and then decreases gradually with higher pH. Therefore, the BR with pH 2.0 was chosen for all experiments.

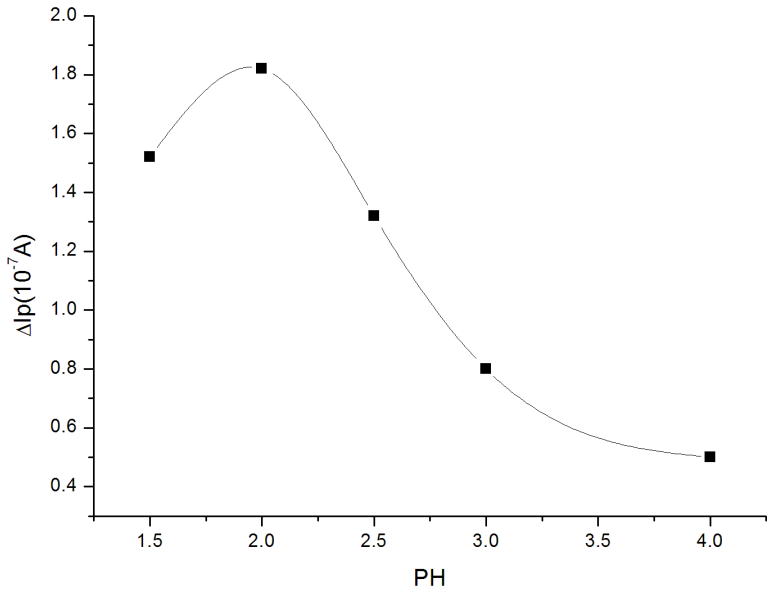

Figure S8. Effects of the pH obtained by the differential pulse voltammograms (DPV) curves of 25.2 μM probe **1** with 1.0 nM GSH in 0.2 M BR buffer solution with different pH at a scan rate of 100 $mV \cdot s^{-1}$. All data were obtained after incubation at 25 °C for 20 min.

4.2 Effect of the Reaction time

The time required for reaction of probe **1** with GSH was investigated by DPV experiment. The measurement was performed by a cathodic DPV scan from 0.3 to -0.4 V at a scan rate of 100 $mV \cdot s^{-1}$ while keeping the reaction temperature constant at 25 ºC. As shown in Fig. S9, when the reaction time ranges from 1 min to 20 min, the ΔI_P of probe **1** increases with reaction time and then levels off at reaction time greater than about 20 min. Therefore, 20 min was essential for the substantially balanced

reaction between probe **1** and GSH.

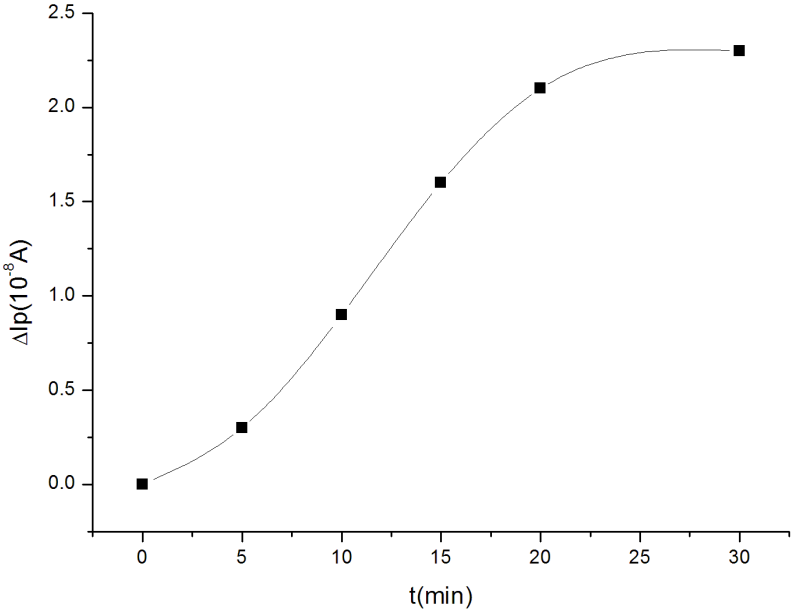

Figure S9. Effects of time obtained by the differential pulse voltammograms (DPV) curves of 25.2 μM probe **1** with 0.1 nM GSH in 0.2 M BR (pH 2.0) at a scan rate of 100 $mV \cdot s^{-1}$.

5. Detection of GSH

Under optimal conditions, 25.2 μM probe **1** was used to detect GSH. The results are shown in Fig.1 and Fig. S10. As shown in Fig. 1, a linear relationship between the ΔI_P of probe **1** and GSH concentration was plotted when the concentration of GSH was in the range of 1.0×10^{-10} to ~1.0×10^{-9} M. The linear regression equation was obtained as: ΔI_P (10^{-7} A) = -0.376 + 0.306×C_{GSH} (10^{-10} M) with the detection limit of 1.0×10^{-10} M (3σ, n = 11). The DPV parameters were as follows: initial potential: 0.3 V; final potential: −0.4 V; scan rate: 100 mV/s.

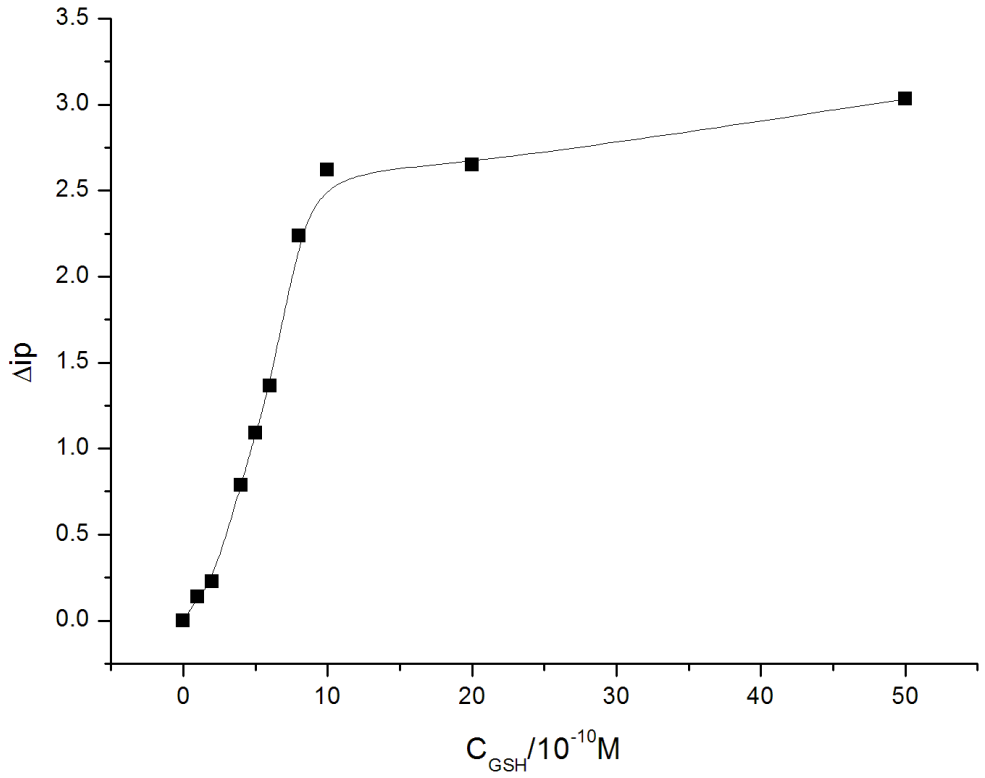

Figure S10. Relationship between the ΔI_P of probe **1** (25.2 μM) and GSH concentration (final concentrations: 0, 0.1, 0.2, 0.4, 0.5, 0.6, 0.8, 1.0, 2.0, 5.0 nM) after incubation at 25 °C for 20 min in 0.2 M BR (pH 2.0).

6. Reactivity of Probe 1 with Thiol-containing Analytes

To evaluate the reactivity of probe **1** with thiol-containing analytes, HS^- and several common non-protein sulfhydryl compounds similar as GSH were studied by measuring the decrease in peak current using 25.2 μM of probe **1** and 5.0 nM of the employed analogues including HS^-, 6-mercapto-1-hexanol (MCH), cysteine (CYS), dithiothreitol (DTT) and thioglycolic acid (TA). As shown in Fig. S11, the probe **1** was observed to show the most sensitive response to GSH than any other studied thiol-containing analytes.

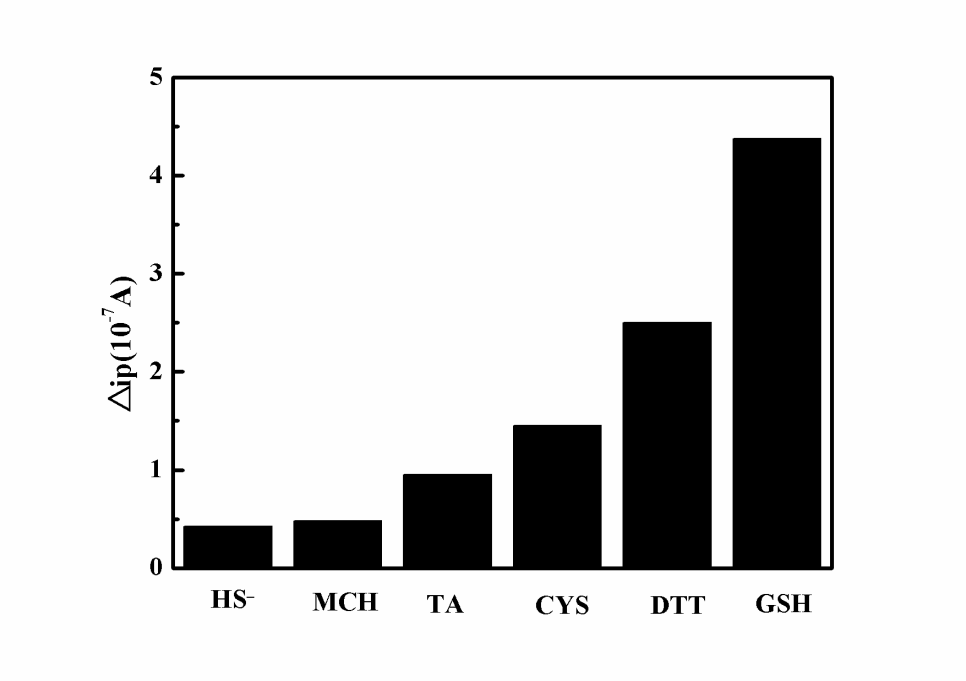

Figure S11. Electrochemical responses of probe **1** (25.2 μM) toward different kinds of thiol-containing analytes (5.0 nM) in BR.

Two protein thiols of metallothionein (MT) and glutathione reductase (GR) were tested. Figure S12 shows the responses of the peak current decreases (Δi_P) of 25.2 μM probe **1** with the addition of MT (Figure S12A) and GR (Figure S12B), respectively. It can be seen that the Δip of probe **1** increased with the concentration of MT, which was varied from 0.01 nM to 5.0 nM and GR from 0.25 mU/L to 100.0 mU/L, respectively, and then reached a platform. It is noteworthy that probe **1** could still achieve sensitive detection even at a low concentration of 0.01 nM MT. Thus, probe **1** is more sensitive to protein thiols than non-protein thiols.

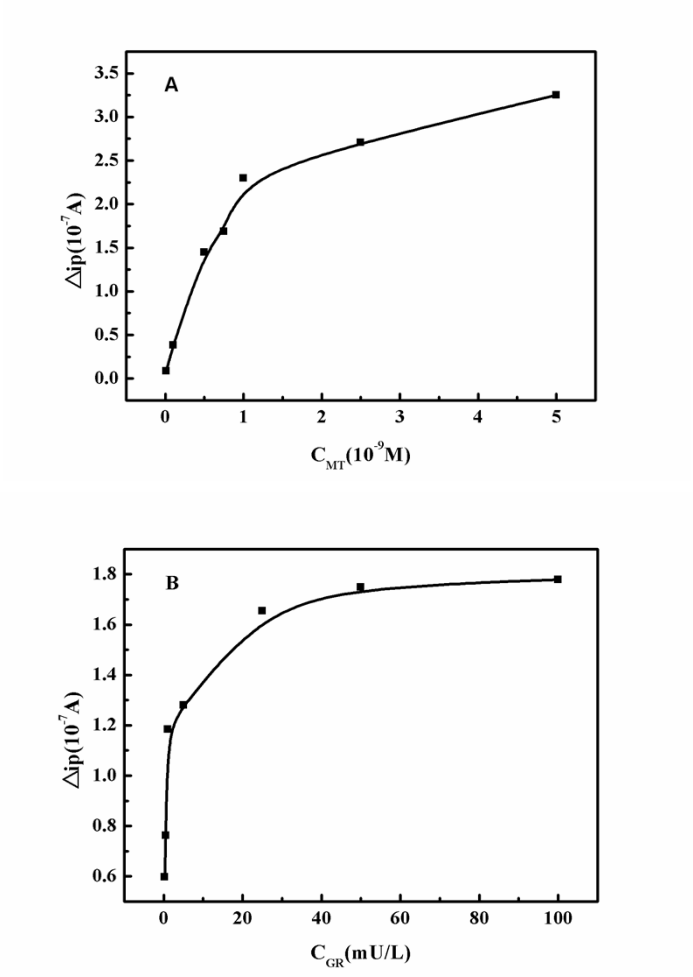

Figure S12. Electrochemical responses of 25.2 μM probe **1** toward (A): MT (0.01, 0.1, 0.5, 0.75, 1.0, 2.5, 5.0 nM); (B): GR (0.25, 0.5, 1.0, 5.0, 25.0, 50.0, 100.0 mU/L) in BR buffer solution (pH 2.0, 0.2 M). All data were obtained after incubation at 25°C for 20 min.

For a comparison, the electrochemical responses of 25.2 μM of probe **1** with the same concentration of MT and GSH were recorded. As shown in Figure S13, protein thiol MT always induced much larger Δip than that of non-protein thiol GSH in three different concentrations. The results are in good agreement with our previous report.

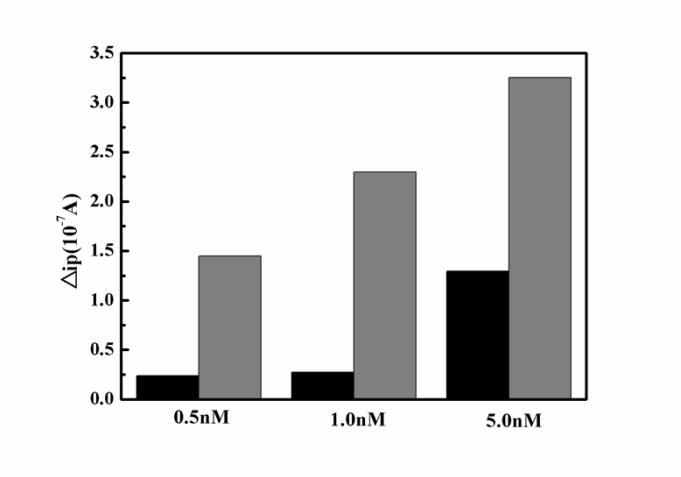

Figure S13. Electrochemical responses of probe **1** (25.2 μM) toward GSH and MT. The black bars represent GSH and the gray bars represent MT.

7. Cell Detection

Ramos cells (a B-cell lymphoma cell line) were used to evaluate the usefulness of the proposed method in actual biological samples. Cells were seeded at a density of 2.0×10^5 cells/mL for intracellular non-protein thiol detection.[7] Cells were resuspended in 3 mL sodium phosphate-EDTA buffer after being washed with ice-cold PBS for three times. A 3% perchloric acid was added into the cell homogenate to precipitate proteins. The supernatant used for detection of non-protein thiols was collected after centrifuging the mixture at 14,000 rpm for 5 min at 4 °C. Each aliquot (10 μL 10-fold diluted supernatant) was mixed with probe **1** (25.2 μM) in 0.2 M BR (pH 2.0) and the other one was pretreated with the thiol-blocking reagent N-ethylmaleimide (NEM, 1.0 mM) for 30 min before reaction with probe **1**. The detection was performed by DPV after reaction for 20 min at 25 °C (Fig. S14).

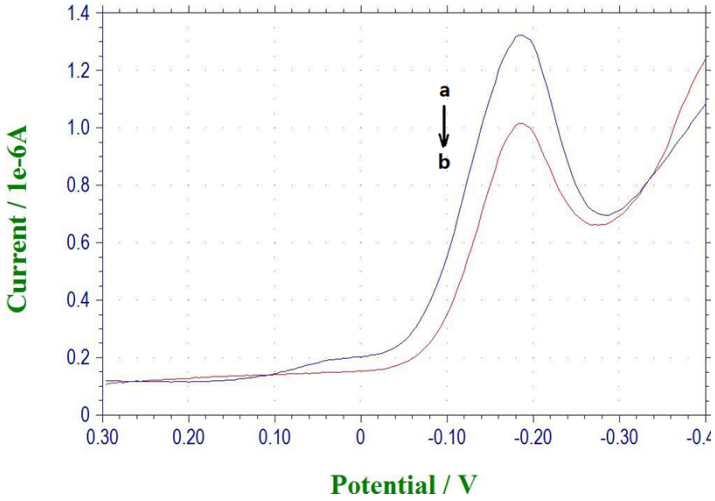

Figure S14. Differential pulse voltammograms of probe **1** (25.2 μM) in the absence (a) and in the presence of non-protein thiols in Ramos cells extracts in BR.

8. Fluorescence Measurements

In order to further explore the application of the probe **1**, the fluorescence measurements were carried out on a Hitachi F-4600 fluorescence spectrophotometer with excitation wavelength at 375 nm. Probe **1** was found to show a fluorescence emission peak at 425 nm in mixture solution of acetone and water. Upon the addition of GSH, the intensity of fluorescence decreased dramatically, which could be ascribed to the consumption reaction of probe **1** with GSH. That is to say, the CT fluorescence decreases due to the nucleophilic reaction of GSH, which results in the transformation of piazselenole to *o*-phenylene-diamine. As indicated in Figure S15, when probe **1** (6.5×10^{-5} M) reacted with different concentrations of GSH, there is a linearity between fluorescence intensity change (ΔF) and the common logarithm of concentrations of GSH in the range of 1.0×10^{-8} - 2.0×10^{-5} M, and the regression equation is $\Delta F = 141.7396 + 14.8171 \times \lg C_{GSH}$ with a linear coefficient of 0.9938. These results indicate that **1** can be used as a fluorescent probe to detect GSH qualitatively and quantitatively.

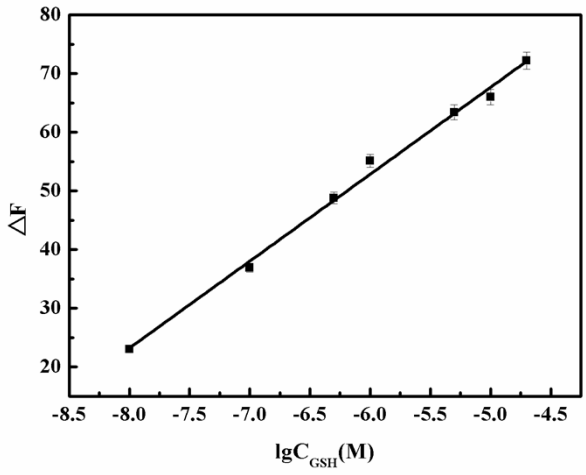

Figure S15. Variation of fluorescence intensity of probe **1** toward the common logarithm of different concentrations of GSH (final concentration: 1.0×10^{-8}, 1.0×10^{-7}, 5.0×10^{-7}, 1.0×10^{-6}, 5.0×10^{-6}, 1.0×10^{-5}, 2.0×10^{-5} M).

References

1 Oxford Diffraction (2010). CrysAlisPro (Version 1.171.34.36). Oxford Diffraction Ltd., Yarnton, Oxfordshire, UK.

2 A. Altomare, M. C. Burla, M. Camalli, G. Cascarano, C. Giacovazzo, A. Guagliardi, A. G. G. Moliterni, G. Polidori and R. Spagna, *J. Appl. Crystallogr.*, 1999, **32**, 115.

3 G. M. Sheldrick, *Acta Cryst.*, 2008, **A64**, 112.

4 C. Jia, S.-X. Liu, C. Tanner, C. Leiggener, A. Neels, L. Sanguinet, E. Levillain, S. Leutwyler, Hauser and S. Decurtins, *Chem. Eur. J.*, 2007, **13**, 3804.

5 (a) J. A. Hansen, J. Becher, J. O. Jeppesen, E. Levillain, M. B. Nielsen, B. M. Petersen, J. C. Petersen and Y. Sahin, *J. Mater. Chem.*, 2004, **14**, 179; (b) N. Svenstrup, K. M. Rasmussen, T. Kruse Hansen and J. Becher, *Synthesis*, 1994, 809.

6 W. Wang, L. Li,. S. Liu, C. Ma and S. Zhang, *J. Am. Chem. Soc.*, 2008, **130**, 10846.

7 C.-F. Yang, H.-M. Shen and C.-N. Ong, *Biochem. Biophys.*, 2000, **374**, 142.